A Simplified Reduced-Dimensionality Study to Treat Reactions of the Type $X + CZ_3Y \rightarrow XY + CZ_3$†

Boutheïna Kerkeni and David C. Clary*

Physical and Theoretical Chemistry Laboratory, Oxford University, South Parks Road, Oxford OX1 3QZ, United Kingdom

Received: March 26, 2003; In Final Form: September 4, 2003

We present calculations on reactions of the type $X + CZ_3Y \rightarrow XY + CZ_3$ using a reduced-dimensionality model with two degrees of freedom. Only the Y−C vibrational mode ν_1 of CZ_3Y and the stretching vibration of X−Y are treated explicitly in the scattering problem. An approximation accounting for the umbrella ν_2 mode of CZ_3 has been introduced. A direct comparison with previous calculations of state-selected reaction cross sections is made on the reactions $O(^3P) + CH_4 \rightarrow OH + CH_3$ and $O(^3P) + CH_3D \rightarrow OD + CH_3$. The results show that the approximation applied, in which the umbrella mode is not accounted for explicitly in the scattering calculations, gives good results for some vibrationally selected reaction cross sections. In agreement with previous results, we find that the umbrella mode is more efficient in promoting the $O(^3P) + CH_4 \rightarrow OH + CH_3$ reaction and that the stretching vibration enhances the $O(^3P) + CH_3D \rightarrow OD + CH_3$ reaction.

1. Introduction

In recent years, reduced-dimensionality (RD) quantum scattering models have been developed to study reactions involving polyatomics. Those models consider a subset of the degrees of freedom and treat them by rigorous quantum methods while accounting for the remaining degrees of freedom by a variety of approximate methods, like the energy-shifting procedures[1−3] and more complex adiabatic treatments.

A number of reactions involving more than four atoms have been studied using RD quantum scattering techniques. These reactions include $OH + CH_4 \rightarrow H_2O + CH_3$,[4,5] $H + C_2H_2 \rightarrow H_2 + C_2H$,[6] $NH_3 + OH \rightarrow NH_2 + H_2O$,[7] $H + CH_4 \rightarrow H_2 + CH_3$,[8] $Cl^- + CH_3Cl \rightarrow ClCH_3 + Cl^-$,[9] and $Cl^- + CH_3Br \rightarrow ClCH_3 + Br^-$.[10]

The rotating bond approximation (RBA)[11−13] enables the selection of degrees of freedom that can be identified with vibrational or rotational modes in both reactants and products.[11] It has been applied to many four-atom polyatomic reactions[11,14] and has been extended to treat the umbrella vibration in the gas-phase S_N2 reactions[9,10,15,16] and the hydrogen abstraction reaction in three- and four-dimensional calculations[17−19] in which the umbrella motion was described as an angular coordinate.

Nyman and Yu (1998)[20] used a related 2D quantum scattering model to derive rate constants for the $Cl + CH_4 \rightarrow HCl + CH_3$ reaction. The model is in essence the rotating linear model (RLM), but it incorporates an adiabatic correction that differs from that used in the bending-corrected rotating linear model (BCRLM).[21,22] In BCRLM, the constructed potential function includes the zero-point energies (ZPEs) of the modes not explicitly treated in the quantum dynamics. Their model was previously used to study the $OH + CH_4 \rightarrow CH_3 + H_2O$ reaction, and it was termed the rotating line approximation (RLA). A comparison with a 3D, RBA model has also been investigated.[23] In the RLA calculation, the H_2O bend was not explicitly treated; the RBA and RLA rate constants were in close agreement when the adiabatic treatment is used for the bending degree of freedom, which is treated explicitly in the RBA but not in the RLA. As an extension to their 2D model, Yu and Nyman[24] developed a three-dimensional model to study again the $Cl + CH_4 \rightarrow HCl + CH_3$ reaction in which the umbrella mode is treated explicitly and was simulated by the vibration of the pseudo-diatom approximation of CH_3, it was termed rotating line umbrella (RLU) model. Furthermore, the authors developed a 4D model termed rotating bond umbrella (RBU) model[25] and applied it first to the $Cl + CH_4 \rightarrow HCl + CH_3$, $H + CH_4 \rightarrow H_2 + CH_3$,[26] and $O + CH_4 \rightarrow OH + CH_3$[27] reactions, in which the zero-point energy of the modes not explicitly treated in the RBU calculations is approximately included. The RBU model includes four internal motions: the two reactive bond stretches, the umbrella vibrational mode, and the rotational mode of CH_3, which becomes a bending mode in CH_4.

Many reliable RD models have been used frequently to study the hydrogen abstraction reactions from methane.[17−20,26−30] Cumulative and state-to-state reaction probabilities, as well as thermal rate constants, were also computed[20,26,28,29] and compared to experimental ones. Time-dependent wave packet calculations were used to obtain reaction probabilities for state-selected reagents.[28,31]

Earlier work[30] on the $O(^3P) + CH_4(s',u') \rightarrow OH(s) + CH_3$ reaction was based on a three-dimensional model (3D, RBA) and treats explicitly the CH_4 umbrella and bending vibrational modes, the CH_3 umbrella mode, and CH_3 rotations. The following studies[17] were based on an extension of that model, using different approaches for treating the umbrella motion. The latest work (4D, RBA)[19] examines the role of the symmetric and asymmetric stretching vibrations of CH_4 on promoting reaction. There are many experimental reports of the rate constant for this reaction.[17,26] The same model was also used later[32] to study the effect of the symmetric and the asymmetric

† Part of the special issue "Charles S. Parmenter Festschrift".

* To whom correspondence should be addressed. Electronic mail: david.clary@chem.ox.ac.uk.

10.1021/jp0303725 CCC: $25.00
Published on Web 11/14/2003

stretching vibrations on the $O(^3P) + CH_3D(s',u') \rightarrow OD(s) + CH_3$ reaction.

It is important to develop RD models that can be evaluated by direct comparisons with experiment or exact state-selected or state-to-state reaction probabilities. This can be achieved by including in the models normal vibrations of the actual molecule[17,19] that do not distort significantly the vibrational modes of reactants and products. The basic idea behind RD models is that just a few degrees of freedom of the reactive system participate actively during the collision process.[1] The others act as spectators to the reaction. Accordingly, only this small number of active degrees of freedom are treated explicitly in close-coupling expansions in quantum scattering calculations. For all of these reasons, in the present study, we introduce an approximation to a previously used (3D, RBA) model[30] and evaluate the reagent state-selected cross sections. This model accounts for one internal degree of freedom; the second is the scattering coordinate. On the reactant side ($X + CZ_3Y$), the method explicitly considers the Y−C vibration s′ of the breaking bond in CZ_3Y, while on the product side ($XY + CZ_3$), only the X−Y vibration s of the forming bond is considered explicitly. The umbrella motion, characterized by the u′ quantum number, was not coupled to the internal degree of freedom in the present calculations. In the 2D model, we evaluate the Hessian matrix of the potential function and add the harmonic frequency of the selected excited umbrella state to the optimized potential during a family of independent calculations, one for each umbrella excited state. This represents an extension of the BCRLM to polyatomic reactions.

We study the following reactions

$$O(^3P) + CH_4(s',u') \rightarrow OH(s) + CH_3 \quad (1)$$

$$O(^3P) + CH_3D(s',u') \rightarrow OD(s) + CH_3 \quad (2)$$

Comparison with the RBA results enables the importance of coupling the umbrella vibration to the scattering coordinate to be examined. We discuss the differences between the present and the previous RD calculations using the same potential energy surfaces (PESs) to facilitate understanding of reaction dynamics of polyatomics. The paper is organized as follows. In section 2, we describe the theory and give some numerical details. In section 3, we show the reaction probabilities and discuss them. Finally, we present our main conclusions in section 4.

2. Theory

We employed the hyperspherical coordinates (ρ,δ) defined in the usual way from the Jacobi R_1 and R_2 coordinates to write the Hamiltonian, perform calculations, and extract the scattering **S**-matrix.[30] The distance joining X and Y atoms is R_2, and the distance between the center of mass of XY and the center of mass of CZ_3 is R_1. The polar hyperspherical coordinates[15,33] are obtained from the following transformation

$$\frac{M_1}{\mu}R_1^{\,2} = [\rho\cos(\delta)]^2$$

$$\frac{M_2}{\mu}R_2^{\,2} = [\rho\sin(\delta)]^2 \quad (3)$$

where M_1, M_2, M_3, and $\mu = (M_1M_2M_3)^{1/3}$ are defined in ref 30. The Hamiltonian for use in our calculations is extracted from the same reference

$$\hat{H} = -\frac{\hbar^2}{2\mu}\frac{\partial^2}{\partial\rho^2} - \frac{\hbar^2}{2\mu\rho^2}\frac{\partial^2}{\partial\delta^2} + \frac{3\hbar^2}{8\mu\rho^2} + \frac{\hbar^2 J(J+1)}{2\mu\rho^2} + V(\rho,\delta,\theta) \quad (4)$$

where J is the total angular momentum quantum number associated with the rotation of $X-Y-CZ_3$ as a rigid linear body and $V(\rho,\delta,\theta)$ is the potential energy surface. θ and the remaining terms are defined in ref 30. The integration procedure is made between ρ_{min} and ρ_{max} over N_γ sectors. For a fixed total energy E and initial quantum state k', the total wave function is expanded in each sector i in the coupled channel form

$$\Psi_{k'}(\rho,\delta;\rho_i) = \sum_s^N f_{sk'}(\rho;\rho_i)\sum_{n_\delta}^{N_\delta} c_{n\delta}^s \psi_{n\delta}^{ref}(\delta;\rho_i) \quad (5)$$

where N is the number of propagated channels and N_δ is the size of the $\psi_{n\delta}^{ref}(\delta;\rho_i)$ basis. ρ_i indicates the value of ρ in the center of the ith sector, and $k' = (s',u')$; s' and u' are the quantum numbers of the stretching and umbrella vibrations of CZ_3Y, respectively.

Equation 5 is equivalent to eq 14 of the 3D, RBA model;[30] however, in this 2D model, the sum is restricted to s vibrational states of products XY rather than the sum over $k = (s, u)$ products vibrational states. The consequence of this new definition of the initial wave function will be discussed in section 3.

$\psi_{n\delta}^{ref}(\delta;\rho_i)$ are the discrete variable representation (DVR)[34,35] eigenvectors of the Hamiltonian

$$H_\delta = -\frac{\hbar^2}{2\mu{\rho_i}^2}\frac{\partial^2}{\partial\delta^2} + V_\delta^{ref}(\delta;\rho_i) \quad (6)$$

The hyperspherical adiabats, $\epsilon_s(\rho_i)$, are the corresponding eigenvalues of this Hamiltonian. They are obtained by using a particle-in-a-box primitive basis set with $0 \le \delta \le \delta_{max}$, $\delta_{max} = \arctan[(m_Y m_{tot}/(m_X(m_C + 3m_Z)))^{1/2}]$ and $m_{tot} = m_X + m_Y + m_{CZ_3}$.

The remaining umbrella degree of freedom θ changes from the reactant side to the product side. The calculation of its frequency was performed around the optimized angle θ_m, and the harmonic potential for the umbrella mode was included adiabatically in the dynamics to account for the zero-point energy. For state-selected umbrella excited reactants (u' quantum number), a reference potential has been introduced. A potential $V_0(\delta;\rho_i)$ was obtained by minimizing the potential energy $V(\delta,\rho_i,\theta)$ with respect to θ for each value of δ. At the optimized structure, the second derivative of the potential energy function with respect to the nuclear angle θ was calculated by numerical differentiation. Finally, the force constant matrix $\kappa_{u'}$ gives the umbrella harmonic frequency

$$\omega_{u'}(\delta;\rho_i) = \sqrt{\frac{\kappa_{u'}}{3m_H{r_{CH}}^2}}$$

For $u' \ge 0$, the reference potential is

$$V_\delta^{ref}(\delta;\rho_i) = V_0(\delta;\rho_i) + \hbar\omega_{u'}(\delta;\rho_i)\left(u' + \frac{1}{2}\right) \quad (7)$$

Note that the umbrella adiabatic eigenvalues form an effective potential, which, when added to the minimized potential $V_0(\delta;\rho_i)$ in each sector i, forms the reference potential of eq 7.

The treatment of the umbrella degree of freedom within this adiabatic approach required a family of calculations of the **S**-matrix for a given u' value, one for each umbrella state. The adiabats are solutions of the Hamiltonian of eq 6 with the

TABLE 1: Values of the Parameters Used in the Scattering Calculations[a]

	reaction	
	1	2
N	10	10
N_δ	120	120
N_γ	235	202
ρ_{min}	6.5	4.8
ρ_{max}	30	25
ρ_a	24	20
ρ_b	30	25
J_{max}	200	200

[a] Distances are in atomic units.

reference potential defined by eq 7. The overlap matrix and the adiabats are stored to be used for higher angular momentum J as described in ref 36. At large values of ρ, the asymptotic wave functions $\psi_{n\delta}^{ref}(\delta;\rho_i)$ become eigenstates of either of the channels X + $CZ_3Y(s',u')$ or XY(s) + CZ_3. We used the expectation value of

$$\langle \psi_{n\delta}^{ref}(\delta;\rho_i)|\delta|\psi_{n\delta}^{ref}(\delta;\rho_i)\rangle \tag{8}$$

to classify the asymptotic reactant and product states. In matrix form, the reactive equations are expressed simply by

$$\frac{d^2}{d\rho^2} f(\rho;\rho_i) + \mathbf{W}(\rho_i) f(\rho;\rho_i) = 0 \tag{9}$$

with the diagonal matrix

$$W_{nn'}(\rho_i) = \frac{2\mu}{\hbar^2}\left[E - \epsilon_s(\rho_i) - \frac{3\hbar^2}{8\mu\rho_i^2} - \frac{\hbar^2 J(J+1)}{2\mu\rho_i^2}\right] \tag{10}$$

With addition of the centrifugal term $J(J+1)/(2\mu\rho^2)$ to eq 10, calculations were performed up to a maximum value J_{max} to ensure convergence of cross sections. We used the **R**-matrix propagation method[37] with a constant step to solve eq 9. Approximate boundary conditions are then applied for ρ_i ranging from ρ_a to ρ_b to obtain sector scattering matrix elements $S^J_{n'n,i}(E)$ for each total energy E. Squaring the state-to-state $S^J_{n'n,i}(E)$ elements produces the state-to-state probabilities $P^J_{n'n,i}(E)$. Averaging them over sectors in the asymptotic region gives the state-to-state probabilities $P^J_{n'n}(E)$ for the model. The reagent state-selected cross section for the model was calculated as

$$\sigma_{n'}(E) = \frac{\pi}{\lambda_{n'}^2}\sum_n \sum_{J=0}^{J_{max}} (2J+1) P^J_{n'n}(E) \tag{11}$$

where $\lambda_{n'}^2 = 2\mu_{X,CZ_3Y}(E - \epsilon_{n'})/\hbar^2$, $\lambda_{n'}$ stands for the initial translational wavenumber and $\mu_{X,CZ_3Y} = m_X m_{CZ_3Y}/m_{tot}$.

Numerical parameters used in the calculations are reported in Table 1. For the O(^{3}P) + CH_4 reaction, calculations were performed using the analytical potential surface (APS) of Corchado et al.[38] appropriate for the reaction on the $^3A'$ potential with a classical barrier height of 13.6 kcal mol^{-1}, which is endothermic by 4.9 kcal mol^{-1}. Calculations for the O(^{3}P) + CH_3D reaction were performed using the semiempirical potential surface with symmetry $^3A''$ of Jordan and Gilbert[39] modified by Epsinosa et al.[40] having a classical barrier height of 13.0 kcal mol^{-1}.

3. Results and Discussion

The vibrational frequencies for the present RD model are shown in Tables 2 and 3 for reactions O(^{3}P) + CH_4 and O(^{3}P) + CH_3D, respectively. These results compare favorably with the RBA values. We notice that according to the inequalities of their ground-state energies, the threshold energy for the reaction O(^{3}P) + CH_3D should be lower than that for the reaction O(^{3}P) + CH_4.

TABLE 2: Vibrational Frequencies in cm^{-1}

vibration	RBA[30]	model
umbrella CH_4	1248	1177
umbrella CH_3	517	501
C−H stretch	2772	2732
O−H stretch	3563	3548

TABLE 3: Vibrational Frequencies in cm^{-1}

vibration	model
umbrella CH_3D	1229
umbrella CH_3	546
C−D stretch	2103
O−D stretch	2609

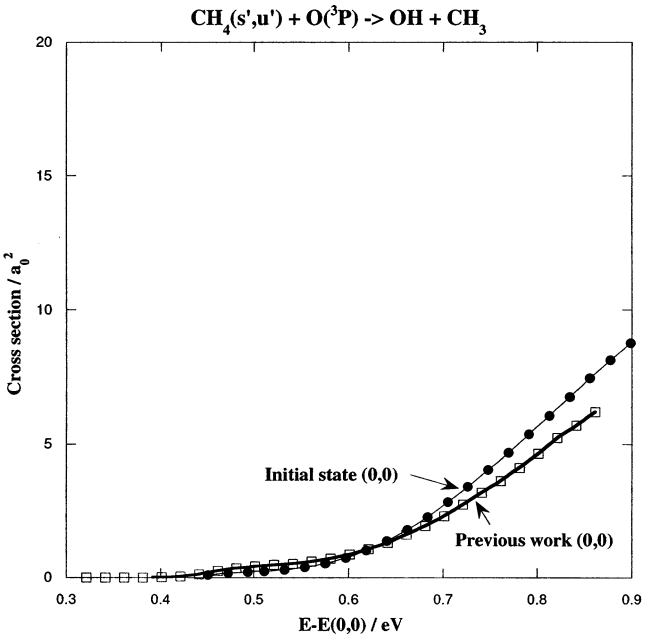

Figure 1. Initial state-selected $CH_4(0,0)$ cross section as a function of translational energy of the ($s' = 0$, $u' = 0$) initial ground state summed over all product states (●) compared to RBA results (□).

3.1. Application to the O(^{3}P) + CH_4(s′,u′) Reaction. In the previous calculations,[17,30] computations were done on the same PES that we have used here and with the wave function $\Psi_k(\delta,\theta;\rho_i)$ expanded in s and u variables (see, eq 14 of ref 30), where $\Psi_k(\delta,\theta;\rho_i)$ can be identified with quantum states of either CH_4 or OH + CH_3 when ρ_i becomes large. Furthermore, it was found in these 3D, RBA calculations that transitions from ($s' = 1$, $u' = 0$) and ($s' = 0$, $u' = 2$) lead to excitations of CH_3 to either $u = 1$ or $u = 2$. Here, we examine the effect of exciting the umbrella and stretching vibrational modes of CH_4 and CH_3D on the reactivity using the model described in section 2.

Results are reported in Figures 1−7 and show the cross sections summed over s product states for the O(^{3}P) + CH_4(s′,u′) reaction as a function of the initial translational energy of the ($s' = 0$, $u' = 0$) state of CH_4. Comparisons between the present calculations and RBA results from ref 30 are also reported. It can be seen in Figure 1 that cross sections out of the ground state ($s' = 0$, $u' = 0$) have the same threshold energy and a similar behavior. The two sets of results show a good

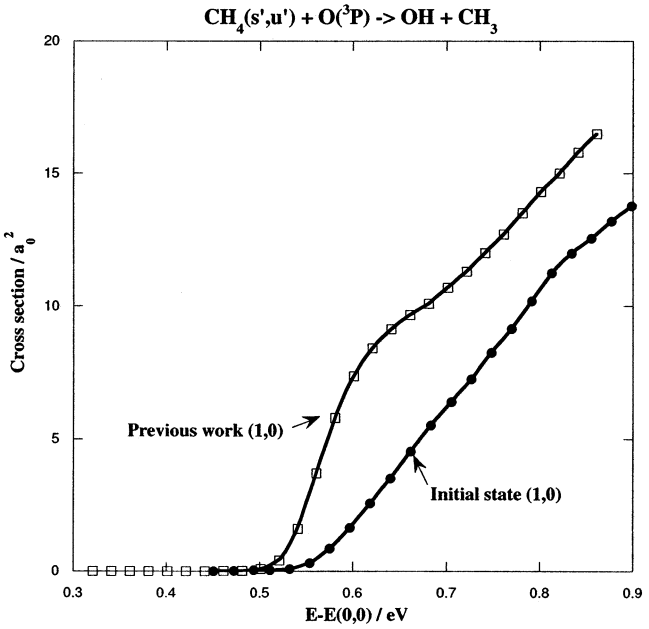

Figure 2. Initial state-selected $CH_4(1,0)$ cross section as a function of translational energy of the ($s' = 0$, $u' = 0$) initial ground state summed over all product states (●) compared to RBA results (□).

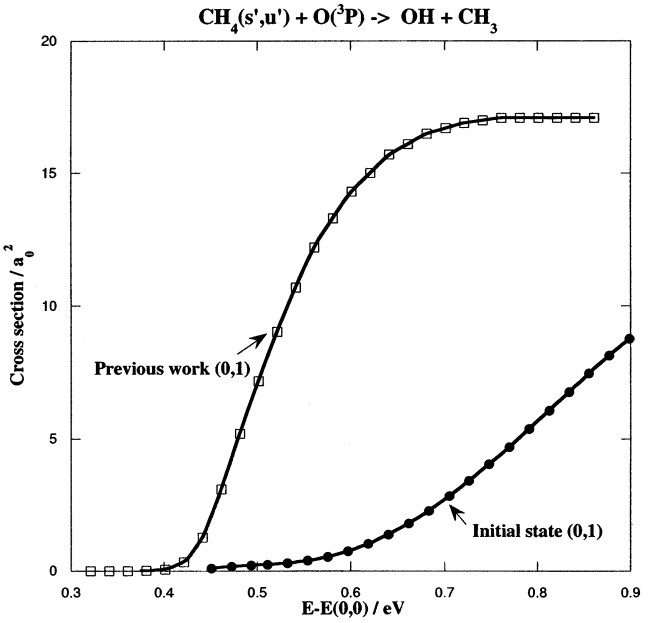

Figure 4. Initial state-selected $CH_4(0,1)$ cross section as a function of translational energy of the ($s' = 0$, $u' = 0$) initial ground state summed over all product states (●) compared to RBA results (□).

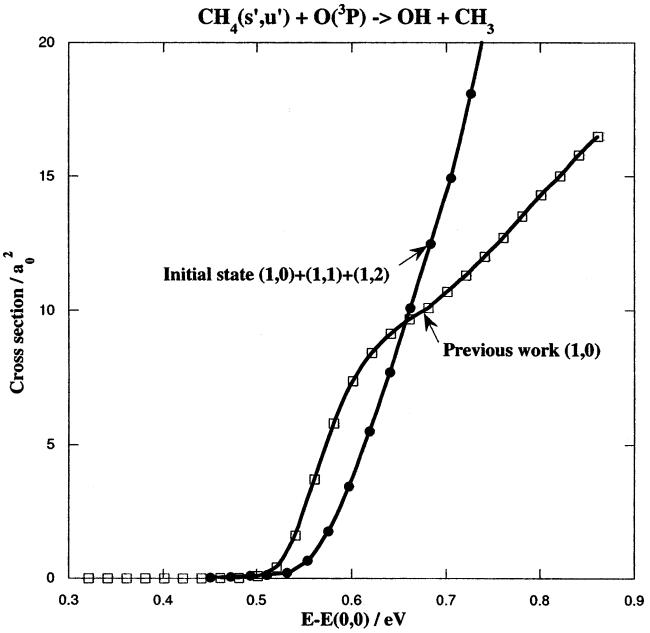

Figure 3. Sum over initial state-selected $CH_4(1,0) + CH_4(1,1) + CH_4(1,2)$ cross sections as a function of translational energy of the ($s' = 0$, $u' = 0$) initial ground state summed over all product states (●) compared to RBA initial state-selected $CH_4(1,0)$ cross section (□).

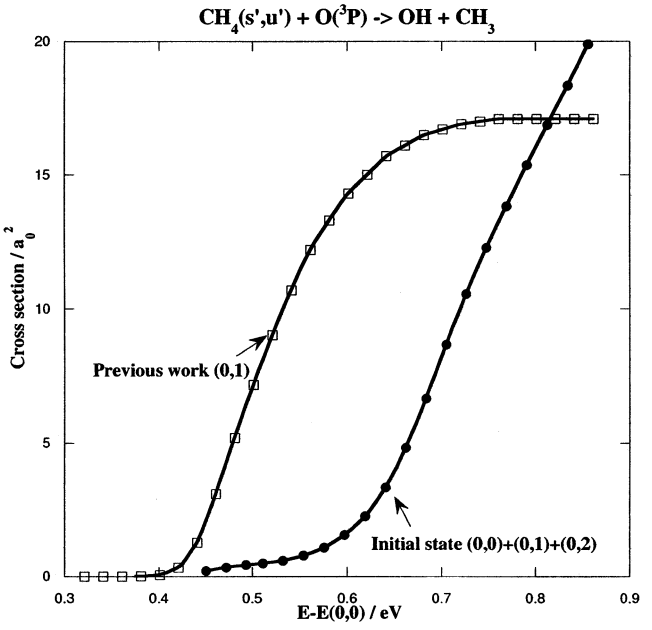

Figure 5. Sum over initial state-selected $CH_4(0,0) + CH_4(0,1) + CH_4(0,2)$ cross sections as a function of translational energy of the ($s' = 0$, $u' = 0$) initial ground state summed over all product states (●) compared to RBA initial state-selected $CH_4(1,0)$ cross section (□).

agreement over the whole energy range. This suggests that the inclusion of the zero-point energy (of the umbrella mode) to the PES has provided an accurate description of the dynamics of umbrella motion especially at threshold.

Cross sections out of ($s' = 1$, $u' = 0$) shown in Figure 2 have the same trend with the previous computations; the 2D cross section is however smaller than the RBA over the whole energy range. Also its threshold is larger than the RBA one. In Figure 3, we plot the cross section obtained by the sum of cross sections out of ($s' = 1$, $u' = 0$), ($s' = 1$, $u' = 1$), and ($s' = 1$, $u' = 2$). This cumulative cross section, accounting for the umbrella mode contribution ($u' = 0$, 1, and 2) from the products compares quite well with the RBA state-selected cross section ($s' = 1$, $u' = 0$) and recovers its effect missing in the total wave function expansion of this 2D model (see eq 5). Because the umbrella motion is treated as if it is adiabatically separable from motion in the (ρ,δ) coordinates, the small difference may be assigned to the neglect of the strong coupling between the stretching mode and the umbrella mode during the reaction.

We present in Figure 4 cross sections from ($s' = 0$, $u' = 1$). This cross section has a large threshold and underestimates the RBA results significantly. However, we show in Figure 5 that the sum over ($s' = 0$, $u' = 0$), ($s' = 0$, $u' = 1$) and ($s' = 0$, $u' = 2$) state-selected cross sections is in slightly better agreement

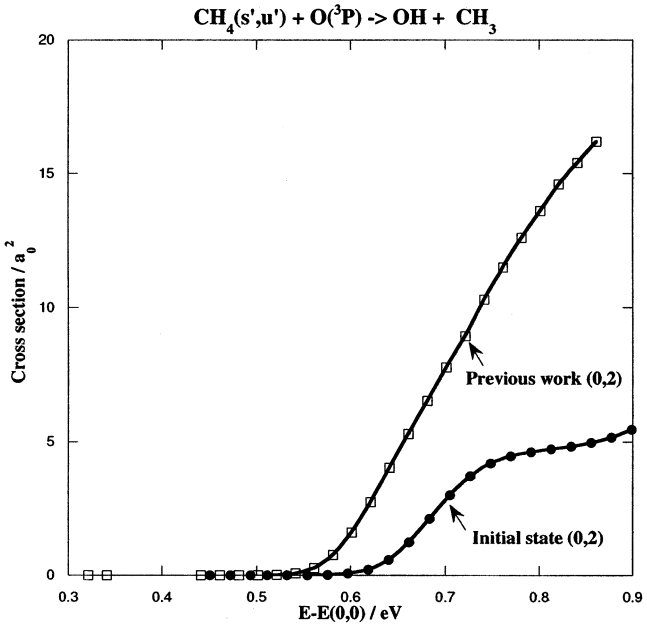

Figure 6. Initial state-selected $CH_4(0,2)$ cross section as a function of translational energy of the ($s' = 0$, $u' = 0$) initial ground state summed over all product states (●) compared to RBA results (□).

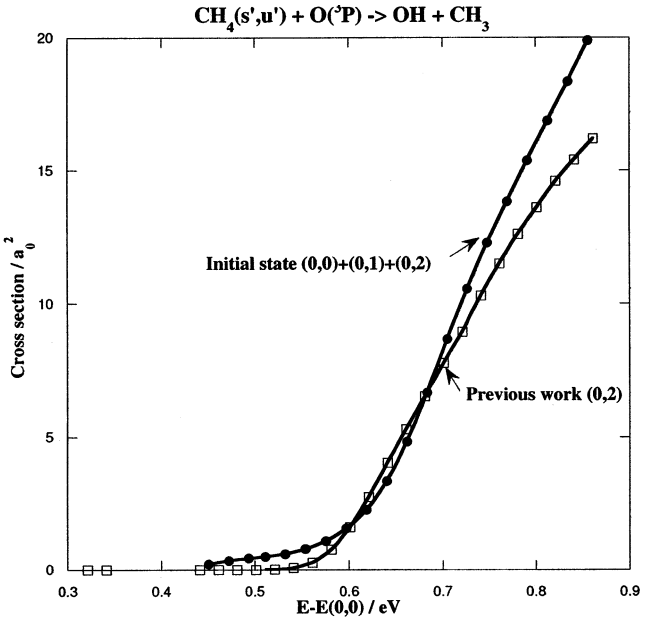

Figure 7. Sum over initial state-selected $CH_4(0,0) + CH_4(0,1) + CH_4(0,2)$ cross sections as a function of translational energy of the ($s' = 0$, $u' = 0$) initial ground state summed over all product states (●) compared to RBA initial state-selected $CH_4(1,0)$ cross section (□).

with the RBA ($s' = 0$, $u' = 1$) result. Cross sections out of the second excited state of the umbrella vibration ($s' = 0$, $u' = 2$) of Figure 6 also underestimate the RBA values and have a large threshold, whereas we see in Figure 7 that the comparison is improved for the cumulative cross sections from ($s' = 0$, $u' = 2$) to ($s' = 0$, all u'). The "umbrella summed" cross sections are closer to the RBA ($s' = 0$, $u' = 2$) state-selected cross sections.

We remark that, apart from the equivalence for the ground-state cross sections with the RBA calculations, only cumulative cross sections (Figures 3, 5, and 7) are close to the 3D, RBA calculations. Cross sections with one quantum of internal excitation in the umbrella mode underestimate the RBA results

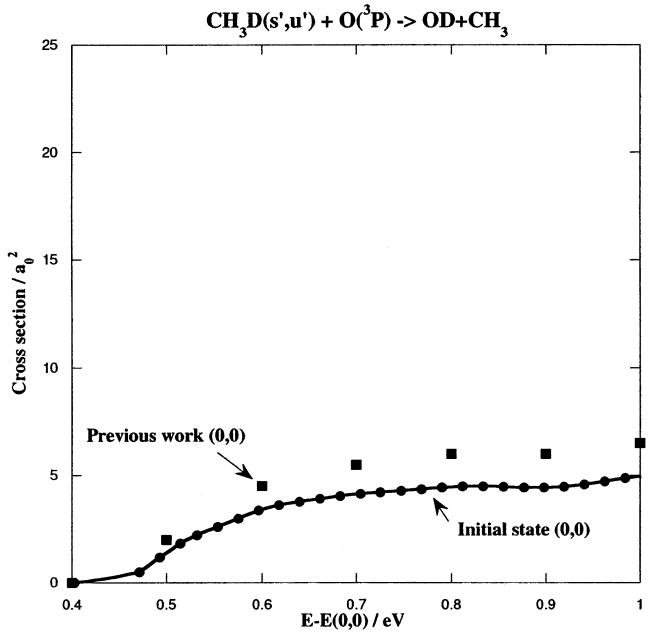

Figure 8. Initial state-selected $CH_3D(0,0)$ cross section as a function of translational energy of the ($s' = 0$, $u' = 0$) initial ground state summed over all product states (●) compared to RBA results (■).

(because the cross sections reported here are only summed over the degrees of freedom explicitly treated in the quantum scattering calculations). A systematic behavior has been underlined, in which state-selected cross sections in (s', u') excited vibrational modes have large thresholds and small contribution when compared to the 3D, RBA model. This reinforces the fact[17,19,30] that the umbrella mode promotes the $O(^3P) + CH_4$ reaction and is strongly coupled with the reaction coordinate and also with the stretching mode.

It is evident that the adiabatic procedure, together with a sum over the state-selected cross sections in the umbrella mode, has improved the comparison between the 2D and the RBA state-selected cross section calculations. This is not surprising because the umbrella degree of freedom does contribute effectively to the progress of the reaction and an explicit treatment is necessary to get a good estimate of the state-selected cross sections.

3.2. Application to $O(^3P) + CH_3D(s',u')$ Reaction. The reagent state-selected cross sections ($s' = 0$, $u' = 0$), ($s' = 1$, $u' = 0$), and ($s' = 0$, $u' = 1$) are plotted versus the initial translational energy of the ($s' = 0$, $u' = 0$) state of CH_3D in Figures 8−10 for the $O(^3P) + CH_3D$ reaction. Comparisons are made with 4D, RBA results from ref 32 from which some values are reported on the plots. We note that the present and RBA cross sections are quite close. They exhibit the same trend and thus provide quite a good agreement for the thermal energy range.

However, the present cross section out of ($s' = 1$, $u' = 0$) is smaller than the RBA at high energies. This result reinforces the fact that the stretching mode has a major effect in promoting this reaction and confirms the strong coupling between the mode promoting the reaction and the remaining modes as was the case for reaction 1 with the umbrella mode. Because the umbrella mode does not have such an important role in this reaction, the state-selected cross sections (in the umbrella u' mode) within this adiabatic approximation describe the dynamics quite accurately.

One could expect that cumulative probability will recover the contribution missing in the state-selected cross sections (in part due to the sum only over explicitly treated degrees of

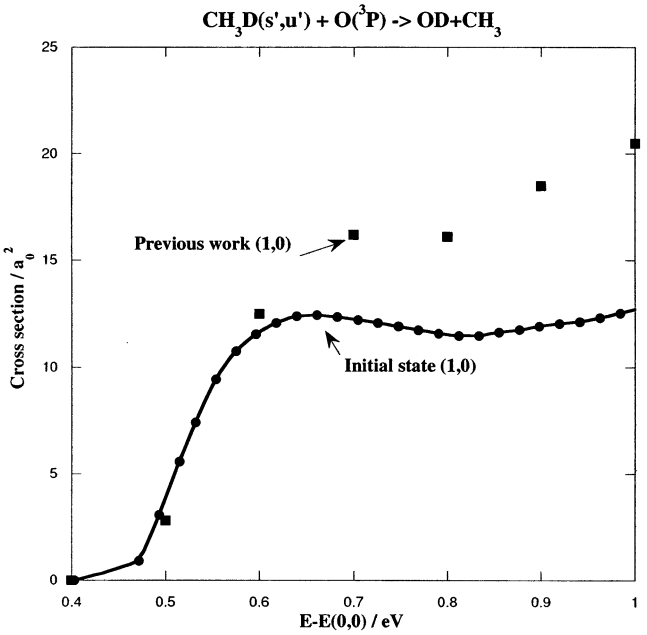

Figure 9. Initial state-selected $CH_3D(1,0)$ cross section as a function of translational energy of the ($s' = 0$, $u' = 0$) initial ground state summed over all product states (●) compared to RBA results (■).

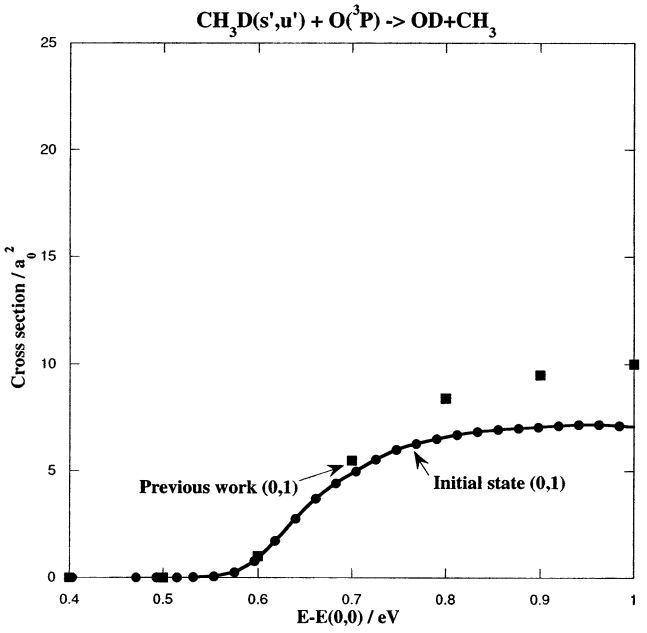

Figure 10. Initial state-selected $CH_3D(0,1)$ cross section as a function of translational energy of the ($s' = 0$, $u' = 0$) initial ground state summed over all product states (●) compared to RBA results (■).

freedom in the definition of the total wave function) and lead to comparable thermal rate constants, when adequate energy-shifting procedures are applied. In the RLA calculations reported by Nyman,[23] on the $OH + CH_4 \rightarrow CH_3 + H_2O$ reaction, the H_2O bending degree of freedom does not contribute effectively to the reaction and hence the RLA cumulative reaction probability and the thermal rate constant agreed well with the 3D, RBA model that treats explicitly the bending mode during the calculations.

4. Conclusions

The principal goal of this paper has been to examine the state-selected dynamics in the reaction of $O(^3P)$ with CH_4 and CH_3D. A reduced-dimensionality quantum-dynamical method has been used in which two stretching vibrations are treated explicitly and the umbrella vibration mode is accounted for by using an adiabatic approximation. Comparison with cross sections obtained with the RBA, in which the umbrella mode is treated explicitly, shows good agreement for transitions out of the ground vibrational states. For transitions from vibrational excited states, the agreement is not so good, especially for CH_4. The results illustrate the significant effect of the umbrella mode on this reaction and suggest that quantum-dynamical calculations that do not treat this mode explicitly should be used with caution.

Acknowledgment. This work was supported by the Engineering and Physical Sciences Research Council.

References and Notes

(1) Bowman, J. M. *J. Phys. Chem.* **1991**, *95*, 4960.
(2) Sun, Q.; Bowman, J. M. *J. Chem. Phys.* **1990**, *92*, 1021.
(3) Sun, Q.; Bowman, J. M. *Int. J. Quantum Chem., Quantum Chem. Symp.* **1989**, *23*, 115.
(4) Nyman, G.; Clary, D. C. *J. Chem. Phys.* **1994**, *101*, 5756.
(5) Nyman, G.; Clary, D. C.; Levine, R. D. *Chem. Phys.* **1995**, *191*, 223.
(6) Wang, D.; Bowman, J. M. *J. Chem. Phys.* **1994**, *101*, 8646.
(7) Nyman, G. *J. Chem. Phys.* **1996**, *104*, 6154.
(8) Takayanagi, T. *J. Chem. Phys.* **1996**, *104*, 2237.
(9) Clary, D. C.; Palma, J. *J. Chem. Phys.* **1997**, *106*, 575.
(10) Garrec, J.-L. L.; Rowe, B. R.; Queffelec, J. L.; Mitchell, J. B. A.; Clary, D. C. *J. Chem. Phys.* **1997**, *107*, 1021.
(11) Clary, D. C. *J. Phys. Chem.* **1994**, *98*, 10678.
(12) Clary, D. C. *Chem. Phys. lett.* **1992**, *34*, 192.
(13) Nyman, G.; Clary, D. C. *J. Chem. Phys.* **1994**, *100*, 3556.
(14) Clary, D. C. *Science* **1998**, *279*, 1879.
(15) Schmatz, S.; Clary, D. C. *J. Chem. Phys.* **1998**, *109*, 8200.
(16) Schmatz, S.; Clary, D. C. *J. Chem. Phys.* **1999**, *110*, 9483.
(17) Palma, J.; Clary, D. C. *J. Chem. Phys.* **1999**, *112*, 1859.
(18) Palma, J.; Clary, D. C. *J. Chem. Phys.* **2001**, *115*, 2188.
(19) Palma, J.; Clary, D. C. *Phys. Chem. Chem. Phys.* **2000**, *2*, 4105.
(20) Nyman, G.; Yu, H. G.; Walker, R. B. *J. Chem. Phys.* **1998**, *109*, 5896.
(21) Walker, R. B.; Hayes, E. F. In *The Theory of Chemical Reaction Dynamics*; Clary, D. C., Ed.; Reidel: Dordrecht, The Netherlands, 1986; p 105.
(22) Hayes, E. F.; Pendergast, P.; Walker, R. B. In *Advances in Molecular Vibrations and Collision Dynamics: Reactive Scattering*. Bowman, J. M., Ed.; JAI: Greenwich, CT, 1994; Vol. 2A.
(23) Nyman, G. *Chem. Phys. Lett.* **1995**, *240*, 571.
(24) Yu, H. G.; Nyman, G. *Phys. Chem. Chem. Phys.* **1999**, *1*, 1181.
(25) Yu, H. G.; Nyman, G. *J. Chem. Phys.* **1999**, *110*, 7233.
(26) Yu, H. G.; Nyman, G. *J. Chem. Phys.* **1999**, *111*, 3508.
(27) Yu, H. G.; Nyman, G. *J. Chem. Phys.* **2000**, *112*, 238.
(28) Wang, M. L.; Li, Y. M.; Zhang, J. Z. H.; Zhang, D. H. *J. Chem. Phys.* **2000**, *113*, 1802.
(29) Wang, D. Y.; Bowman, J. M. *J. Chem. Phys.* **2001**, *115*, 2055.
(30) Clary, D. C. *Phys. Chem. Chem. Phys.* **1999**, *1*, 1173.
(31) Bowman, J. M. *J. Phys. Chem. A* **2001**, *105*, 2502.
(32) Palma, J.; Echave, J.; Clary, D. C. *Chem. Phys. Lett.* **2002**, *363*, 529.
(33) Pack, R. T. *Chem. Phys. Lett.* **1984**, *108*, 333.
(34) Light, J. C.; Hamilton, I. P.; Lill, J. V. *J. Chem. Phys.* **1984**, *82*, 1400.
(35) Muckerman, J. T. *Chem. Phys. Lett.* **1990**, *173*, 200.
(36) Clary, D. C. *J. Chem. Phys.* **1991**, *95*, 7298.
(37) Light, J. C.; Walker, R. B. *J. Chem. Phys.* **1976**, *65*, 4272.
(38) Corchado, J. C.; Espinosa-Garcia, J.; Roberto-Neto, O.; Chuang, Y.-Y.; Truhlar, D. G. *J. Phys. Chem. A* **1998**, *102*, 4899.
(39) Jordan, M. J. T.; Gilbert, R. G. *J. Chem. Phys.* **1995**, *102*, 5669.
(40) Espinosa-Garcia, J.; Garcia-Bernaldez, J. C. *Phys. Chem. Chem. Phys.* **2000**, *2*, 2345.